THE EFFECT OF ELEMENT BOW ON DRYOUT POWER AND POST-DRYOUT HEAT TRANSFER IN CANDU FUEL BUNDLES

S.C. SUTRADHAR and J.R. SCHENK

Fuel Channel Thermalhydraulics Branch
AECL, Chalk River Laboratories
Chalk River, Ontario K0J 1J0

ABSTRACT

Dryout and post-dryout tests were performed in a modified 37-element simulated CANDU fuel bundle, with one outer element of the last bundle bowed at gradual but controlled steps toward the pressure-tube wall. The dryout power decreased moderately as the gap size was reduced from nominal to about 40%. For smaller-than-40%-gap sizes, however, the dryout power increased in most cases; this resulted in almost equal dryout powers at the nominal and zero gap sizes. The maximum surface temperature of the bowed element at up to 20% overpower increased with decreasing gap sizes; however, for gap sizes smaller than 35% of the nominal gap, the surface temperature fluctuated moderately.

INTRODUCTION

Individual elements within a fuel bundle may distort because of a number of mechanisms, either within the fuel element or external to it. One mode of distortion is element bowing, either toward an adjacent element or toward the pressure tube. Bowing may occur because of the differential thermal expansion caused by large circumferential temperature gradients (because of neutron-flux variation) across an element, inadequate fuel-to-coolant heat transfer, irregular subchannel geometries, etc.

During small break loss-of-coolant accidents (LOCAs) in a CANDU reactor, non-uniform fuel heatup at or near nominal element powers over an extended period of time may lead to a distortion of a fuel element. A severely distorted element can cause (i) localized pressure-tube overheating, (ii) sheath failure or (iii) permanent element deformation or both (ii) and (iii).

As an element distorts, coolant circulation around it can vary significantly. The heat-transfer coefficient may deteriorate locally, leading to an escalation in circumferential temperature gradient across the element. If the element is exposed to the significant temperature gradient in the post-dryout condition, permanent deformation or damage may occur. The permanently deformed element could potentially affect the bundle critical heat flux (CHF) during subsequent reactor operation.

To improve our knowledge of dryout behaviour and variation in surface temperature around a severely distorted element, several tests were performed at the Chalk River Laboratories

(CRL) first in water using annular test sections. Because these tests in a simple geometry do not represent the complex flow phenomena in real bundles, CHF and PDO tests in a modified 37-element simulated CANDU fuel string were performed at CRL. One outer element of the last bundle was bowed at gradual but controlled steps toward the pressure-tube wall. Both dryout power and PDO surface-temperature data were obtained using Freon-134a refrigerant as the coolant.

This paper presents the effect of a bowed outer element on CHF of a modified 37-element simulated CANDU fuel bundle, as well as the effect of bow on element surface-temperature distributions at PDO conditions. The data from this and subsequent tests will be used to validate relevant prediction techniques applicable to CANDU fuel bundles. Since the experiments were performed in a modified bundle geometry, the conclusions from this test are not directly applicable to a regular CANDU fuel bundle.

EXPERIMENTAL APPARATUS AND PROCEDURE

Loop Facility

The MR-3 Freon Heat-Transfer Loop at CRL allows heat-transfer tests to be performed on a string of 12 full-scale CANDU fuel bundles. Freon-134a (DuPont tradename for tetra-fluoroethane) cools the test section at a much lower pressure, temperature and power, thus reducing cost and time relative to water tests. Liquid refrigerant circulates at a measured and controlled rate, temperature and pressure through the vertical test section. The test section is heated by a continuously adjustable dc power supply (maximum 1 200 kW).

Test Section

The test section was a 37-element, 12-bundle CANDU fuel string, including end plates, bearing pads and inter-element spacings. One outer element (# 8 in Figure 1) of the last bundle was modified for the test. The element had 8% higher heat flux, over 1.5-m length, than did the other elements in the outer ring, and this modification ensured initial dryout to occur on the intended element. The element was slightly prebowed and the location of maximum bow was 80 mm from the downstream end of the bundle. This location was also the point of closest approach to the tube wall. The bearing pads on the bowed element were removed to facilitate a radial travel of the element. The bundle string, otherwise, had a uniform axial heat-flux distribution, and a natural-uranium (NU) radial heat-flux profile.

The desired gap size between the bowed element and the pressure-tube wall was obtained by moving the element in radial direction, using a cam-drive mechanism. The mechanism was positioned downstream of the bundle string to circumvent any interference with the thermalhydraulic phenomena around the bowed element. The accurately calibrated smooth cam was mounted on the central element and downstream of the last end plate. A solid rod through the copper extension tube above the central element connected the cam to an electric motor, and the motor was positioned outside of the test section.

A transverse push rod, attached to the upstream end of the copper extension rod of the bowed element, glided smoothly over the cam. As the cam was rotated, the push rod moved the bowed element out and in, depending on the direction of cam rotation. Once the element moved close to the tube wall, an electrically activated small brass disc, mounted flushed with the tube wall, indicated its contact with the wall. At this point, further bowing of the bowed element was halted.

Before inserting the bundle string along with the bowed element mounted on the last bundle, the radial movement of the bowed element was calibrated against the angular rotation of the cam. The bundle string was then inserted fully inside the flow tube and the bowed element was slowly brought in contact with the tube wall. The contact signal went off when the element touched the brass disc on the tube wall. The nominal gap between the bowed element and the pressure-tube wall, corresponding to the angular rotation of the cam, was read from the calibration chart. The nominal gap was also the maximum travel of the bowed element during experiment. All gap sizes were measured at the maximum bow location

Sliding thermocouples in the bowed and in 4 surrounding elements (7, 9, 23 and 24 in Figure 1) of the last bundle recorded their surface temperatures. Axial travel of thermocouples in each element was from 16.0 mm, measured from the end of the bundle, up to about half-bundle length, and their angular rotation was 180° (for two diagonally opposing thermocouples in each element). The zero-degree line on the elements was radially outward and closest to the tube wall. The direction of thermocouple rotation was clockwise, looking upstream along individual elements.

Test Procedure

Six equally spaced gap sizes, including the nominal (1.07 mm or 100% gap) and zero gaps, were tested for dryout power at 1.65 MPa pressure, 10 to 16 kg/s flow rate and 40 to 54°C inlet temperature. The PDO tests were performed at 20% overpower, 10.5 kg/s flow rate, 54°C inlet temperature and for 4 equally spaced gap sizes.

Initial dryout power: For the nominal gap size and a selected test condition, the test-section power was increased in small steps to the anticipated dryout power. The bowed element and 4 of its neighbouring elements were scanned thoroughly for the initial dryout at each power increment. The initial dryout power was recorded corresponding to a 5 to 7°C jump in surface temperature of an element. Then the test-section power was reduced slightly (2 to 5 kW). Any variations in the loop conditions from the selected test conditions were re-set, and the power was raised slowly to confirm the initial dryout. At this point, the on-line data acquisition system recorded the pre-assigned test parameters. Then, the gap size was changed and the procedure was repeated.

PDO temperature distribution: For the nominal gap size and a selected flow condition, the test-section power was raised to the initial dryout power. Then the power was increased by 20% beyond the initial dryout power. Thermocouple readings of the bowed element and its surrounding 4 elements were recorded at 40-mm-axial and 30°-angular intervals. Next, the gap size was changed and the surface temperatures were recorded at the same axial and angular intervals.

Several video terminals in the control room displayed various test parameters such as operating pressure, coolant temperature, flow and test-section power. Test-section thermocouple readings, element-to-pressure-tube gap, axial and angular positions of thermocouples, etc., were monitored on separate video terminals.

Additionally, the information about cam rotation, gap size, contact indication, thermocouple positioning, etc., was recorded. Three scans (1 scan per second) were recorded, as well as printed during dryout tests. For PDO tests, however, 1 scan for each thermocouple position was recorded.

RESULTS AND DISCUSSION

Effect of Nominal Gap on Initial Dryout Power

For the nominal (1.07 mm or 100%) gap between the bowed element and the pressure-tube wall, the initial dryout occurred mostly in the vicinity of maximum bow. This was due to the fact that (i) the bowed element had about 8% higher heat flux than did the remaining outer elements, (ii) it had no bearing pads, and (iii) 1.07-mm gap was the smallest gap in the bundle. The extra 8% heat flux was considered to be the dominant factor among the others.

The initial dryout for the nominal gap size was detected along a narrow strip of $\pm 5°$ angular and 50-mm (30 to 80 mm from the downstream end of the bundle) axial spread on the bowed element. The initial dryout power of the bundle string varied linearly with the coolant inlet temperature. High-mass-flow runs required high powers at dryout. Similarly, the initial dryout power decreased almost linearly with the increasing dryout quality (about 12 to 25%) of the bundle string.

Effect of Bowing on Initial Dryout Power

As the gap was reduced progressively from the nominal gap size, the location of dryout moved along the narrow strip, facing the wall, on the bowed element. For the nominal to 40% gap size, dryout occurred usually at and downstream of the point of closest approach for all the runs. The angular spread of the strip was $\pm 15°$.

A further reduction of the gap size (from 40% to zero or contact condition) caused the onset of dryout location to shift upstream of the point of closest approach. The shift was again along the narrow strip facing the flow tube. The axial spread was about 120 mm (80 to 200 mm upstream of the last endplate) for all the runs. The angular spread was the same as in the large gap (nominal to 40%) runs. For either the large or small gap size, no other region of the bowed element, or any other element of the bundle, experienced dryout.

The variation in dryout power with changing gap sizes is shown in Figures 2, 3 and 4, respectively, for 40°C, 47°C and 54°C inlet temperatures. The results for 3 flow rates are plotted in each figure. The figures show that the dryout power decreased for the nominal and up to about 40% gap sizes. This trend, however, reversed as the gap was reduced further.

The minimum dryout power was only 3% (average) lower than the nominal-gap dryout power. But the zero-gap dryout power was almost equal to the nominal-gap dryout power (only -1% average change). This implies that there is no significant change in dryout power of the bundle with decreasing element-to-pressure-tube gap sizes. (Note: Analysis of the test results is continuing and will be published separately.)

Effect of Bowing on PDO Temperature Distribution

Post dryout tests were performed at 20% higher power than that needed to cause the initial dryout on the bowed element at the nominal gap size, and at the test conditions of 10.5 kg/s flow rate, 54°C inlet temperature and 1.65 MPa outlet pressure. The PDO surface temperatures for the bowed element and 4 of its surrounding elements were recorded at 4 gap sizes between the bowed element and the pressure-tube wall.

The temperature contours for the bowed element at different axial locations are plotted in Figures 5 to 8. The dry patch enlarged with increasing overpower. The angular spread was about 180°, and the axial spread was approximately 230 mm. The hottest spot was located along the 0/360° line.

For the nominal gap size, a temperature of 100°C was recorded at 65 mm from the last endplate (Figure 5). Surface temperature reached 120°C as the gap size was reduced further (Figures 6 and 7). The location of the maximum temperature also moved upstream for 65% and 35% gap sizes. As the element was brought very close to the wall (5% gap), the temperature decreased (Figure 8). The location of the maximum temperature moved slightly downstream, from that shown in the previous figures, for the near-wall gap size case. In Figures 5 to 8, the temperature profiles are slightly asymmetric about 180° angular position. This is because of the slight asymmetry in element 8 which was fabricated from commercial tubing.

The surface temperature for small gap sizes (35% and 5% gap sizes) fluctuated mildly along a narrow strip (±30° angular spread) facing the pressure-tube wall. The different points along the 0/360° line for these gaps (in Figures 7 and 8) indicate the fluctuations. The fluctuations could be due to alternating dryout and rewetting at the narrow gap region.

At about 18% overpower, dryout spread to a neighbouring element (# 7 in Figure 1) and the maximum temperature on that element occurred at 65 mm upstream of the last end plate, almost at the same axial location as on the bowed element, for the nominal gap size. The dryout on element 7 occurred on the surface facing the wall subchannel formed by this element, the bowed element and the tube wall. Dry patch on element 7 was smaller compared to that on the bowed element. As the bowed element progressively moved toward the tube wall, the gap between this element and element 7 changed. However, the surface temperature of element 7 did not change significantly with changing gap sizes.

FINAL REMARKS AND CONCLUSIONS

Dryout and PDO tests were performed in a modified 37-element simulated CANDU fuel string cooled by Freon-134a. One outer element (# 8) of the last bundle was bowed at gradual but controlled steps toward the pressure-tube wall. That element, devoid of bearing pads, had 8% higher heat flux than did the remaining outer elements. The element was slightly prebowed, maximum bow was 80 mm upstream of the last end plate. The conclusions are

(a) For the nominal (1.07 mm) gap size, dryout occurred on the bowed element along a narrow strip in the vicinity of maximum bow. The axial spread of dryout was from 30 to 80 mm upstream of the last end plate, and the angular spread was $\pm 5°$. The dryout power decreased linearly with increasing inlet temperature as well as with increasing dryout quality.

(b) The initial dryout for all gap sizes occurred along the narrow strip, facing the flow tube, on the bowed element. For nominal to about 40% gap sizes, the initial dryout appeared downstream of the maximum bow location, whereas dryout moved upstream for 40% to zero gap sizes.

(c) Element bow did not significantly affect initial dryout power of the bundle. The dryout power decreased moderately (3% average decrease) for nominal to 40% gap sizes; it, however, increased for small gap sizes (40% to contact). The increase was small, so that the dryout powers were almost equal (-1% average change) at the nominal and zero gap sizes.

(d) For PDO runs, the dry patch appeared on the surface, facing the tube wall, on the bowed element (# 8). The dry-patch area increased with increasing overpower. About 18% overpower caused a neighbouring element (# 7) to dry out. No other element dried out at or below this overpower.

(e) The maximum surface temperature of the bowed element at PDO conditions increased proportionately with decreasing gap sizes; however, for gap sizes smaller than 35% of the nominal gap, the surface temperature fluctuated moderately. The bowing of an outer element did not significantly affect the temperature distribution of the neighbouring elements.

ACKNOWLEDGEMENTS

The authors would like to acknowledge the funding provided by COG and AECL for this work. The authors would like to thank J.A. Whelan, M.E. Rodych, R.J. Cowhey, B.J. Addicott, J.W. Martin and W.A. McGillis for their support during assembly and test, and S.T. Yin, D.C. Groeneveld and K.F. Rudzinski for their valuable comments and suggestions.

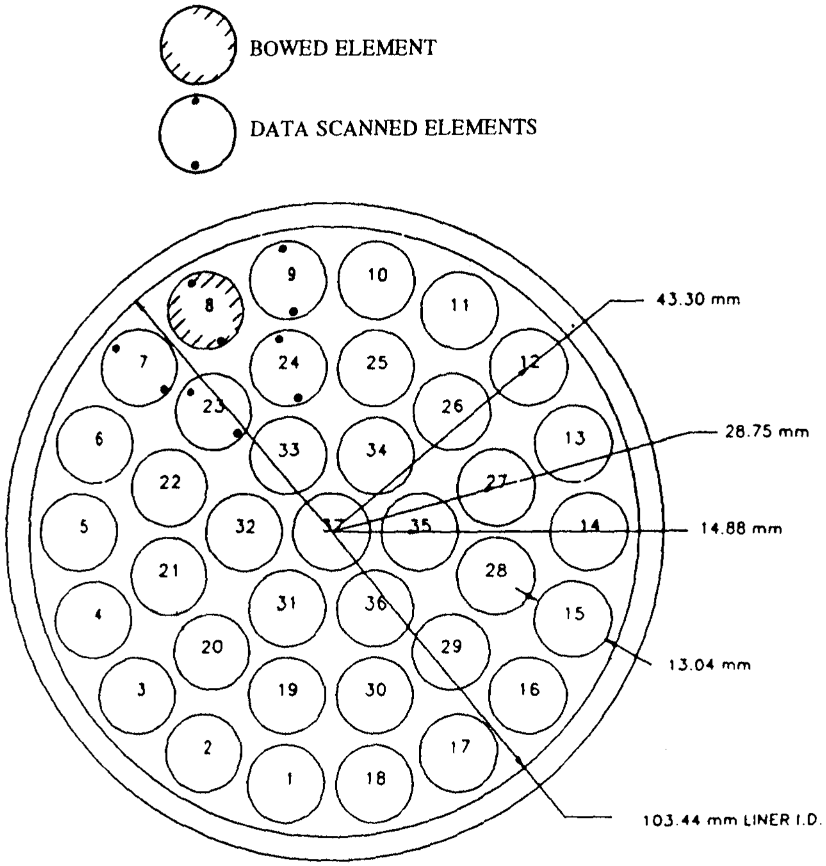

FIGURE 1: CROSS SECTION OF 37-ELEMENT BUNDLE WITH ELEMENT NUMBERS
(looking upstream of test section)

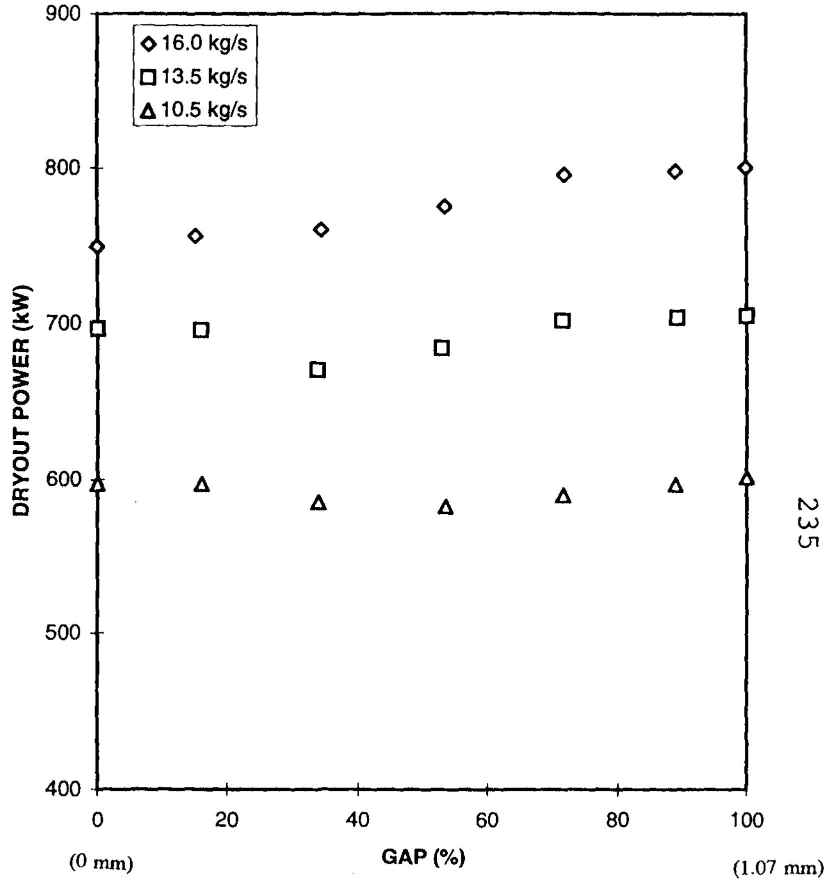

FIGURE 2: VARIATION OF DRYOUT POWER WITH GAP FOR $40^{o}C$ INLET TEMPERATURE AND 1.65 MPa PRESSURE

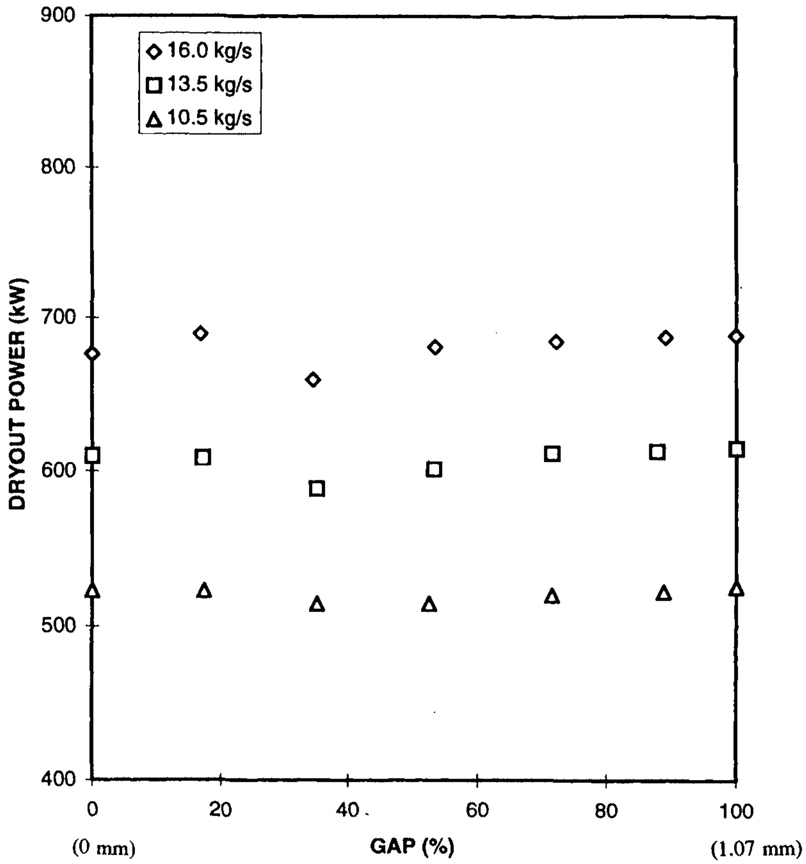

FIGURE 3: VARIATION OF DRYOUT POWER WITH GAP FOR 47°C INLET TEMPERATURE AND 1.65 MPa PRESSURE

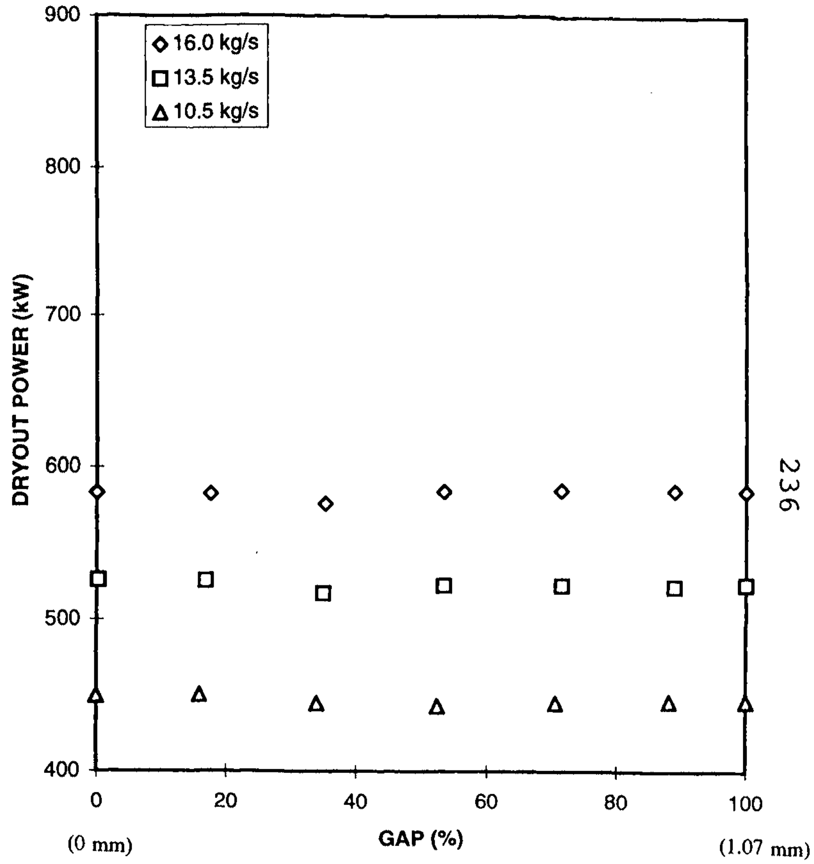

FIGURE 4: VARIATION OF DRYOUT POWER WITH GAP FOR 54°C INLET TEMPERATURE AND 1.65 MPa PRESSURE

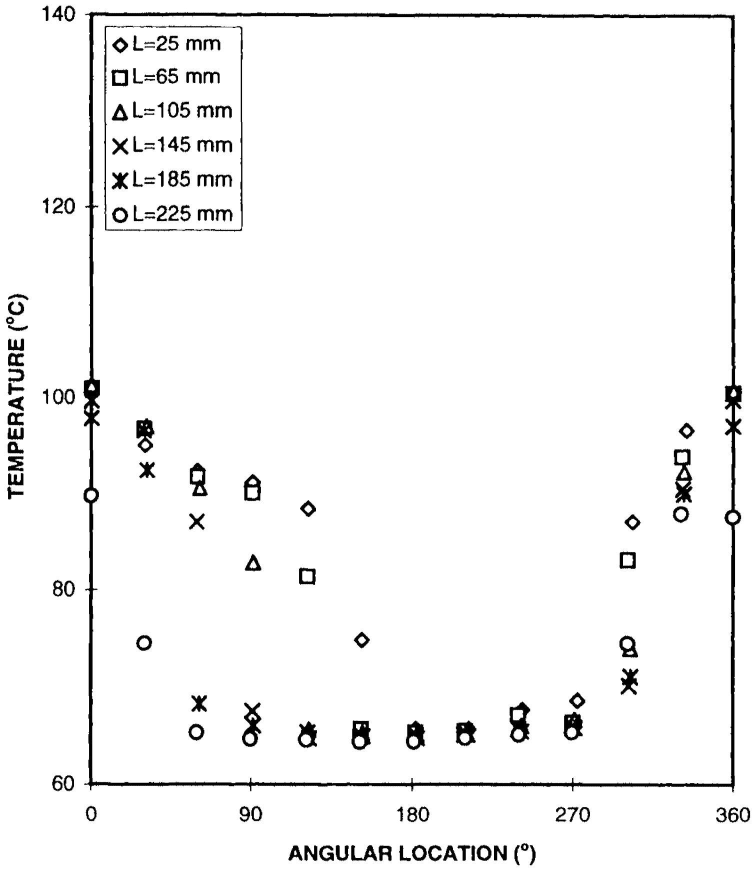

FIGURE 5: SURFACE TEMPERATURE OF THE BOWED ELEMENT
AT 20% OVERPOWER AND AT NOMINAL GAP SIZE
(1.65 MPa pressure., 10.5 kg/s flow rate and 54°C inlet temperature)

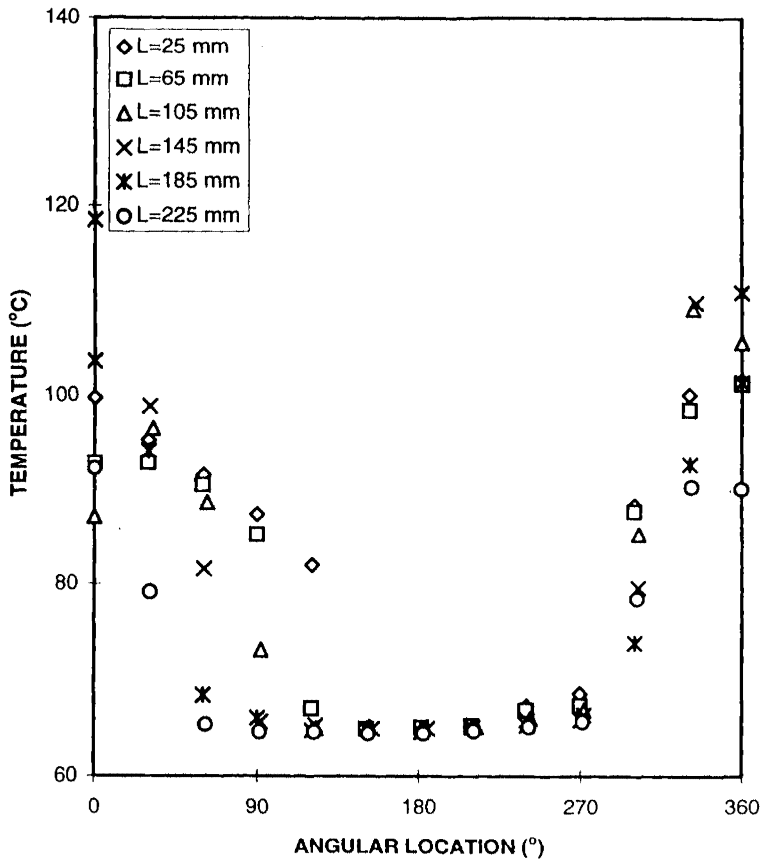

FIGURE 6: SURFACE TEMPERATURE OF THE BOWED ELEMENT
AT 20% OVERPOWER AND AT 65% GAP SIZE
(1.65 MPa pressure., 10.5 kg/s flow rate and 54°C inlet temperature)

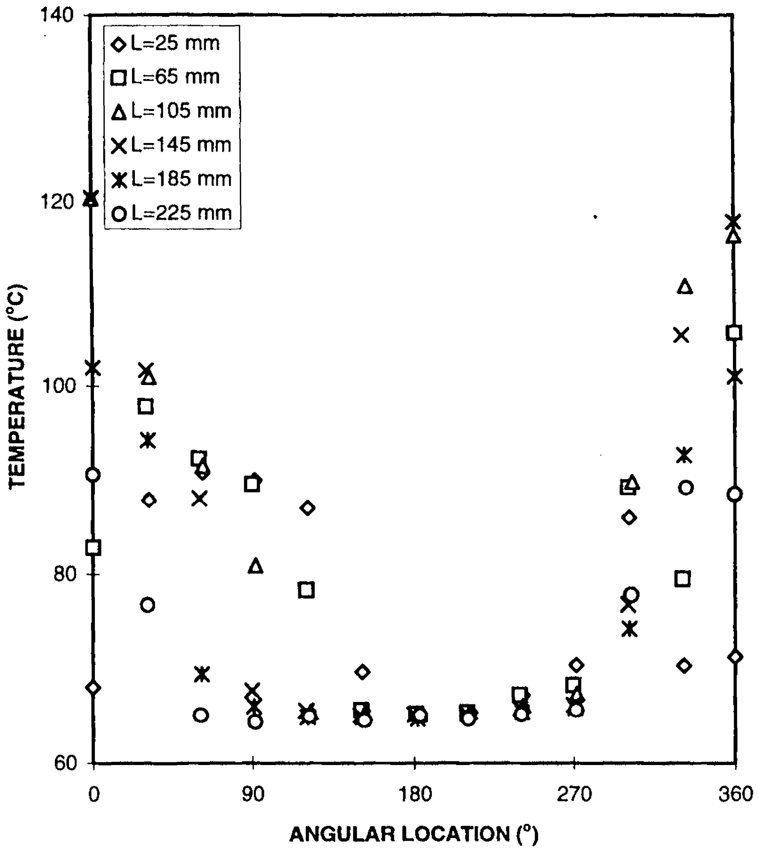

FIGURE 7: SURFACE TEMPERATURE OF THE BOWED ELEMENT
AT 20% OVERPOWER AND AT 35% GAP SIZE
(1.65 MPa pressure., 10.5 kg/s flow rate and 54°C inlet temperature)

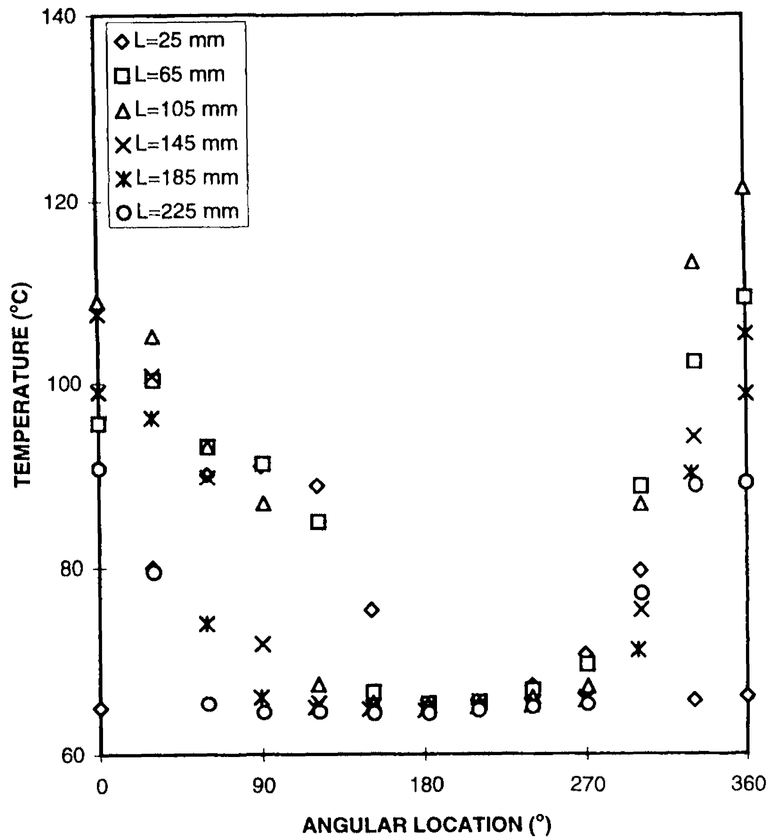

FIGURE 8: SURFACE TEMPERATURE OF THE BOWED ELEMENT
AT 20% OVERPOWER AND AT 5% GAP SIZE
(1.65 MPa pressure., 10.5 kg/s flow rate and 54°C inlet temperature)